Available online at www.sciencedirect.com

ScienceDirect

Current Opinion in Electrochemistry

Review Article

Real-time absorption spectroelectrochemistry: From solution to monolayer

Olivier Alévêque, Christelle Gautier and Eric Levillain

Summary

High-sensitivity charge coupled-device (CCD) cameras, efficient fibre optic bundles, high stable light source and 3D printing technologies now open large possibilities to probe redox species in solution and on confined surface by real-time absorption spectroelectrochemistry. This short review aims at providing an overview of the first work of absorption spectroelectrochemistry on redox-responsive self-assembled monolayers (SAMs). Some practical aspects are emphasized to not underestimate the difficulties involved in set-up such instrumentation.

Addresses

Univ Angers, CNRS UMR 6200, Laboratoire MOLTECH-Anjou, 2 bd Lavoisier, 49045, Angers Cedex, France

Corresponding author: Levillain, Eric (eric.levillain@univ-angers.fr)

Current Opinion in Electrochemistry 2019, **15**:34–41

This review comes from a themed issue on **Organic and molecular electrochemistry**

Edited by **Marc Robert**

For a complete overview see the Issue and the Editorial

Available online 6 April 2019

https://doi.org/10.1016/j.coelec.2019.03.015

Introduction

Electronic (UV-visible and near-infrared (NIR)) transmission and reflectance spectroelectrochemistry (SEC) already proved to be an effective approach for studying the redox chemistry of organic, inorganic and biological compounds. The *in situ* simultaneous acquisition of spectroscopic and electrochemical information in an electrochemical cell (*i.e.* real-time SEC) for investigating reaction kinetics and mechanisms and exploring electrode surface phenomena indeed has a long-standing history [1–9]. The pioneering work was published in 1964 by Kuwana et al. [10], who reported a true technical feat for their time: the use of the SnO_2 electrode to monitor the absorbance during electrolysis at a given wavelength. Half a century later, the improvement in CCD cameras (*i.e.* very sensitive and stable with low noise and large dynamics), light sources (*i.e.* stability *vs.* time), fibre optic bundles and 3D printing technologies has paved the way for the development of very efficient real-time SEC capable of probing redox-response nanomaterials at high sampling rate (*e.g.* 1 optical spectrum per millisecond with a high signal-to-noise ratio). By the way, León and Mozo [11] provide a recent review dedicated to SEC and some major breakthroughs in the field with more than 300 references.

In this short review, the first paragraph reminds some practical but essential aspects of real-time absorption SEC (A-SEC) for monitoring very low absorbance values. Then, a second paragraph will be dedicated to a textbook case A-SEC response: a perylenediimide (PDI) redox probe in solution and immobilized on Au substrate. Finally, the last paragraph gathers the very first results of A-SEC on self-assembled monolayers (SAMs) extracted from the literature.

A few practical reminders

In solution, Beer's law defines the usual relationship between concentration and absorbance as follows:

$A = \varepsilon \ell C$ with ε, the extinction coefficient (mol^{-1} L cm^{-1}); ℓ, the path length (cm) and C, the concentration (mol L^{-1}).

For redox-responsive materials (*e.g.* a SAM), Beer's law can be expressed as follows:

$A = 1000\ \varepsilon_{APP}\ \Gamma$ with Γ, the surface coverage (mol cm^{-2}) and ε_{APP} the apparent extinction coefficient of the material.

It is generally accepted that ε_{APP} depends on the average tilt angle of immobilized molecules (*i.e.* the average dipole moment orientation *vs.* the light beam direction, perpendicular to the substrate), and readers should keep in mind that, in a borderline case, a zero value of tilt angle induces a zero value of ε_{APP} [12–21]. Consequently, the measured absorbance is highly structure dependent of the material.

Probing a SAM by A-SEC imposes to deal with very low absorbance values, close to 0.001 (with

Figure 1

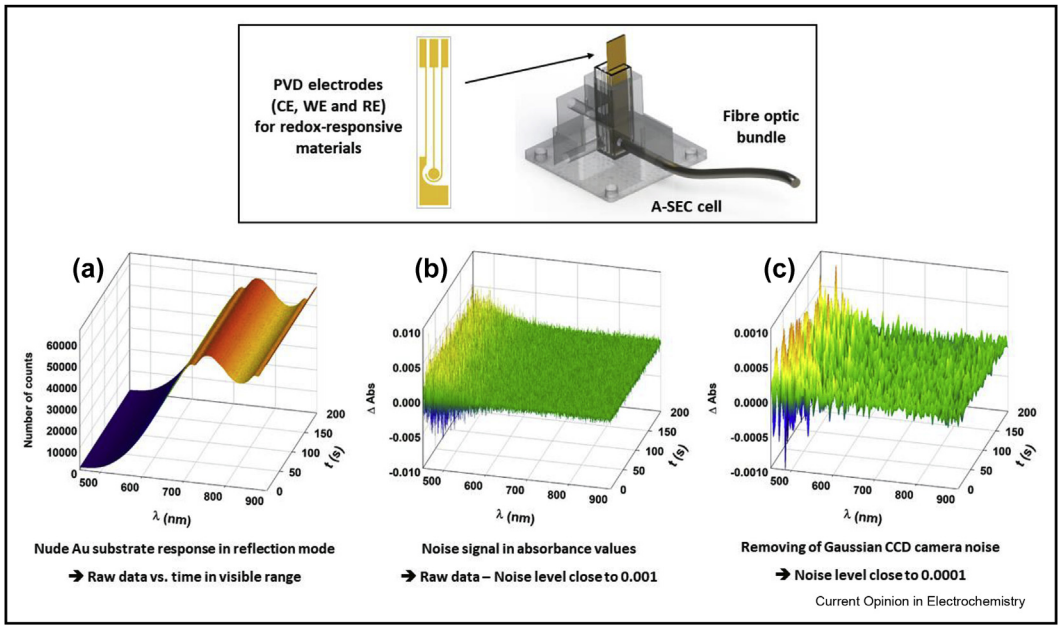

(Top) A-SEC cell dedicated to redox-responsive materials: Disposable electrodes are made by physical vapour deposition (PVD), leading to a reproducible geometry and low roughness (*i.e.* Ra ≈ 2 nm). Produced by a 3D printer, the cuvette holder is designed to minimize the light signal attenuation and accommodate the electrode placement in the optical cuvette, thereby offering a perpendicular light path for reflection and fluorescence measurements. **(a)** (Bottom) Repeatability of the A-SEC bench on nude Au substrate versus time: the numbers of counts (I) measured by the CCD camera are monitored over time (*i.e.* 200 s at a sampling rate of 100 Hz) in real-time A-SEC conditions (3D graph). Note that the number of counts depends on the wavelength range. **(b)** The values of the absorbance variation over the whole wavelength range (*i.e.* 450–900 nm) are calculated from the usual equation $\Delta Abs = \log(I_0/I)$ with I_0, the average of all the frames. The noise level reaches a wavelength-dependent value close to 0.001 (3D graph). **(c)** According to experimental data, the Gaussian noise can be removed via some specific 2D convolution operators to reach a noise level 10 times lower than the previous one (3D graph). Note that the reliability and relevance of this procedure are highly dependent on the sensitivity of CCD cameras, the quality of the calibrations and the maintenance of the A-SEC bench. A-SEC, absorption spectroelectrochemistry; CE, counter electrode; WE, working electrode; RE, reference electrode; CCD, charge coupled-device.

$\Gamma \approx 10^{-10}$ mol cm^{-2} and $\varepsilon_{APP} = 10\,000$ mol^{-1} L cm^{-1}). This challenge seems huge, but performing A-SEC in thin layer conditions can be equally problematic because all measurements need to be, at each step of potential, in an effective steady state to correlate spectroscopic and electrochemical data. In this case, a quite short conversion time (t) close to 1 s imposes a thin layer thickness (ℓ) of about ten micrometres (with $\ell < (t.D)^{1/2}$ and a diffusion coefficient D of *ca* 5.10^{-6} cm^2 s^{-1}), resulting in low absorbance values (*e.g.* A = 0.01 with $\varepsilon = 10\,000$ mol^{-1} L cm^{-1}, $\ell = 10$ µm and C = 1 mM) [6]. It should be noted that A-SEC on the SAM can lead to unusual hardships when the substrate strongly absorbs photon from the light source (*e.g.* vitreous carbon). In such a case, a careful spectroelectrochemical study of nonfunctionalised working electrodes is required to prevent unexpected signals, which could result in misleading or inaccurate interpretations.

In addition, it should also be kept in mind that, under such conditions, performing A-SEC in transmission mode has proven, so far, to be very difficult via a commercial or homemade thin layer cyclic voltammetry (TLCV) cell because ℓ is at best close to 200 µm. Therefore, a reflection mode turns out to be a method of choice because it (i) provides an optimal control of the optical path length (via a micrometric screw, a spacer and so on), (ii) doubles the absorbance (*i.e.* the light beam passes through the thin film twice, meaning that $A = 2\,\varepsilon\,\ell\,C$), (iii) minimizes the light signal attenuation and, the icing on the cake, (iv) enables photoluminescence monitoring via perpendicular excitation to the electrode surface by real-time emission SEC (E-SEC) [22–25]. By the way, a recent review of Bizzotto [26] provides a general overview of E-SEC on the SAM.

Last but not least, a high-sensitivity CCD camera with a signal-to-noise ratio (S/N) above 1000 (i.e. S/N = (Gain. I)$^{1/2}$ with I, the number of counts and Gain, the conversion between the number of electrons recorded by the CCD and the number of digital units contained in

the CCD image) and a high stable light source over time are required to monitor such extremely low absorbance variation. Moreover, the large dynamic range of up-to-date CCD cameras leads to sampling frequencies around a few megahertz (on 16 or 32 bits) and thus a real-time monitoring of redox process and possible chemical reactions accompanying it on millisecond scale or even less. However, reaching such a time scale strongly depends on CCD camera settings, and a compromise between the number of points and the lag time is required to optimize either the dynamics or the sensitivity.

One last point that is often problematic is as follows: the choice of reference spectrum (*i.e.* the radiant flux I_0 [λ] received by the sample) is crucial to extract very low absorbance or transmittance values because real-time A-SEC imposes a single-beam scanning bench. To minimize the noise propagation, the radiant flux I_0 must be at the steady state (*e.g.* I_0 = an average of the first measured frames), and thus, A-SEC experiments monitor an absorbance variation (ΔA) and not an absorbance value (i.e. $\Delta A = \log (I/I_0) = A - A_0$ with A_0 = absorbance at steady state). Consequently, an electrochemical consumption of a steady-state species results in a negative absorbance and the generation of a redox species, and products arising from redox reaction leads to a positive one.

Nowadays, a fine-tuned real-time spectroelectrochemical bench, equipped with the aforementioned instrumentation, allows optical spectra to be monitored at high sampling rate (typically between 10 and 100 Hz at 100 mV s^{-1} for cyclic voltammetry (CV) experiments) with experimental noise lower than 0.0005 (Figure 1).

A-SEC of PDI derivatives, a textbook case

A PDI derivative, known to be an efficient redox chromophore, is suitable for illustrating the procedure for performing A-SEC on the SAM. At this stage, it is worth remembering that, before probing an electroactive SAM by A-SEC, the molecule has to be studied first in solution.

In nonaqueous solvents, PDI derivatives exhibit two successive fully reversible one-electron processes in negative direction, absorb most visible light in the blue

Figure 2

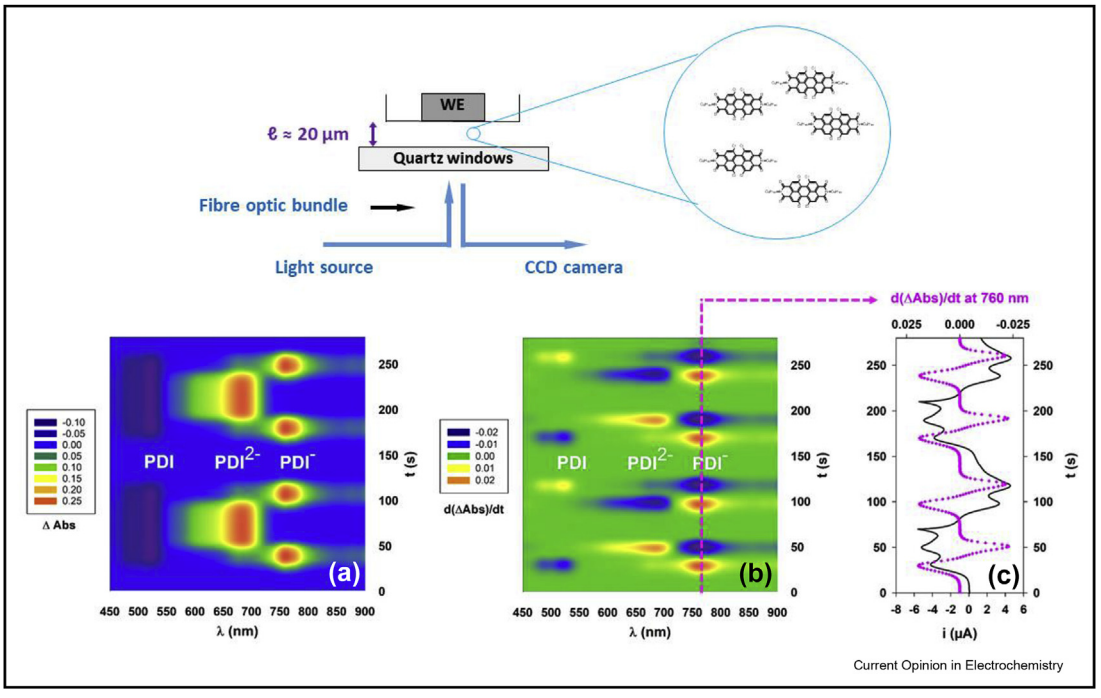

Schematic layout of real-time A-SEC in reflection mode for monitoring spectroelectrochemical behaviour in solution (top). (a) A-SEC response at a sampling rate of 5 Hz of a PDI derivative in nonaqueous solvents, exhibiting two successive reductions in thin layer conditions ($\ell \approx 20$ mm, C = 1 mM in 0.1 M TBAHP/CH_2Cl_2 on Pt electrode at 5 mV s^{-1}). Note that an electrochemical consumption of a steady-state species leads to observation of negative absorbance and vice versa (reminder: ΔA = A - A0 and consequently $d(\Delta A)/dt = d(A)/dt$). (b) First-time derivative of the absorbance variation of A-SEC response, allowing the extraction of all the DCVAs over wavelength (see, for instance, the extraction at 760 nm on (c)) and, thereby, facilitating an effective assignation of the optical bands monitored during the two reduction processes of PDI in solution. (c) Current vs. time on two electrochemical cycles and DCVA at 760 nm. Note that a colour scale represents the 3D graph z-axis. [22]. A-SEC, absorption spectroelectrochemistry; DCVA, derivative cyclic voltabsorptogram; PDI, perylenediimide; CCD, charge coupled-device; TBAHP, tetrabutylammonium hexafluorophosphate.

and green regions (*i.e.* λ_{max} between 450 and 500 nm with a ε of *ca* 40 000 mol^{-1} L cm^{-1}) and produce green light when excited at λ_{max} with a photoluminescence quantum yield close to 100%. A-SEC in thin layer conditions at several scan rates and concentrations may help to check the absence of any homogeneous or heterogeneous reactions coupled to charge transfer while identifying the spectral signatures of the radical anion and dianion arising from the reduction of PDI in solution (Figure 2) [22,23].

Several synthesis steps are required to afford graftable PDI derivatives involved in the formation of PDI-based SAMs on Au substrates. Furthermore, the chemical and electrochemical stability of redox-responsive nanomaterials must be ensured to avoid any molecular desorption during A-SEC experiments. The absence of mass transfer by diffusion in the SAM allows performance of fast and reliable A-SEC experiments in a large range of scan rates and facilitates the monitoring of optical spectra of redox species and/or products arising from redox reactions. The sensitivity of CCD cameras and the high signal-to-noise ratio make the derivative cyclic voltabsorptogram (DCVA) possible on the SAM in a large range of surface coverage (Figure 3) [27].

The study of mixed PDI-based SAMs by A-SEC revealed a Beer's law issue (Figure 4). The absorbance maxima of PDI species indeed vary nonlinearly with surface coverage. In other words, the more the surface coverage increases, the more the absorbance deviates from Beer's law, which has been interpreted (but still not confirmed so far) by surface coverage dependence of the tilt angle of PDI moieties, inducing a direction change of dipolar moments [28].

Decreasing the number of PDI immobilized onto surface induced by the formation of mixed PDI-based SAMs provided an estimation of the detection limit in absorbance value. According to the wavelength range (from 320

Figure 3

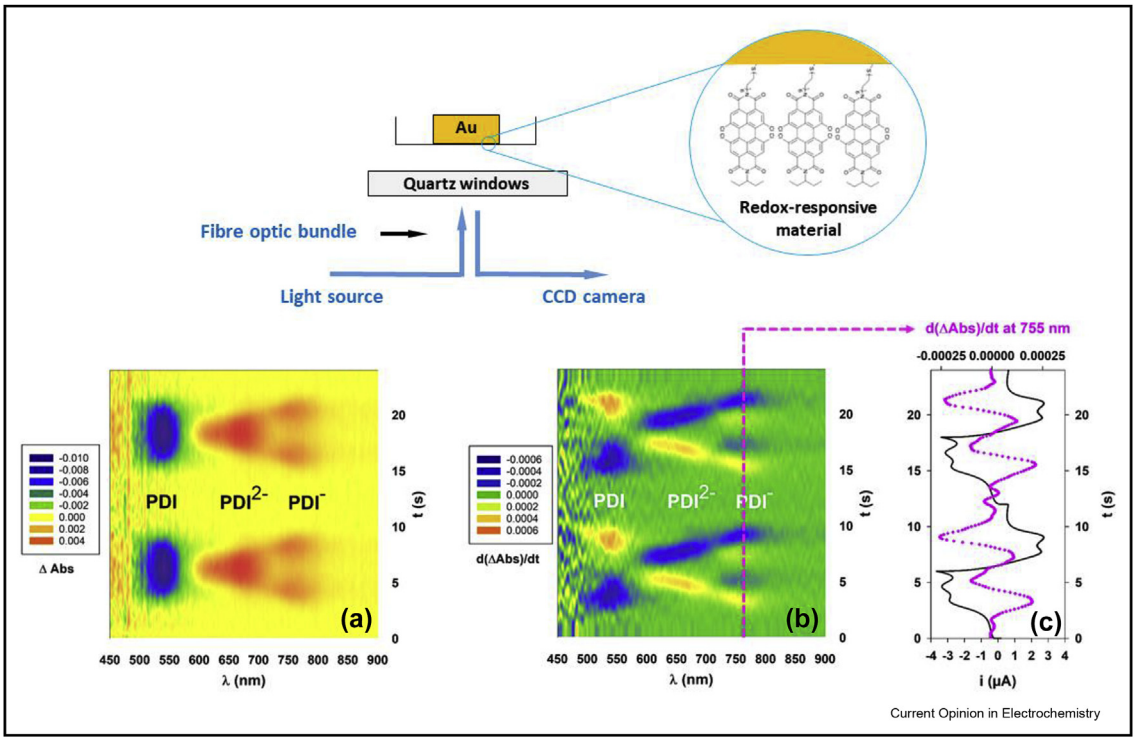

Schematic layout of real-time A-SEC in reflection mode for monitoring spectroelectrochemical behaviour of surface-confined redox species (top). (a) A-SEC response at a sampling rate of 100 Hz of a PDI based SAM in nonaqueous solvents, exhibiting two successive reductions ($\Gamma \approx 2\ 10^{-10}$ mol cm^{-2} in 0.1 M TBAHP/CH_2Cl_2 on Au electrode at 100 mV s^{-1}). Note that an electrochemical consumption of a steady-state species leads to observation of negative absorbance and vice versa (reminder: ΔA = A - A0 and consequently d(ΔA)/dt = d(A)/dt). (b) First-time derivative of the absorbance variation of A-SEC response allowing the extraction of all the DCVAs over wavelength (see, for instance, the extraction at 755 nm on (C)) and, thereby, facilitating an effective assignation of the optical bands monitored during the two reduction processes of PDI in solution. (c) Current vs. time on two electrochemical cycles and DCVA at 760 nm. Note that a colour scale represents the 3D graph z-axis. [27]. A-SEC, absorption spectroelectrochemistry; DCVA, derivative cyclic voltabsorptogram; PDI, perylenediimide; SAM, self-assembled monolayer; CCD, charge coupled-device; TBAHP, tetrabutylammonium hexafluorophosphate.

Figure 4

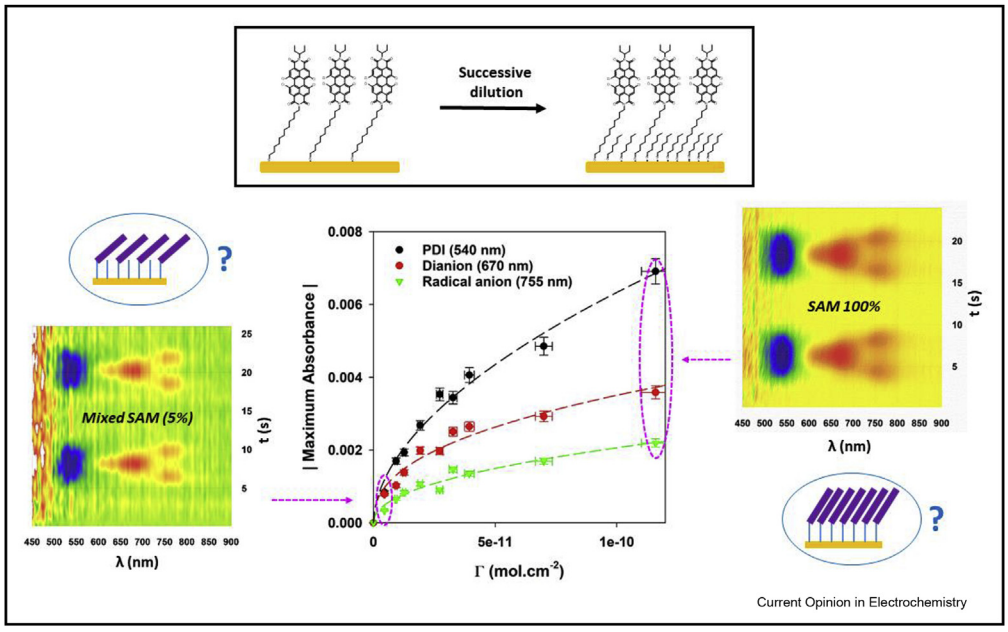

Maximum absorbance at 540, 670 and 755 nm has been extracted from A-SEC experiments of mixed SAMs in 0.1 M TBAHP/CH_2Cl_2 at 10 mV s^{-1} and 303 K. The dash lines are trend curves. Note that the experimental absorbance values at 540 nm (*i.e.* PDI) are negative, but they are displayed in absolute value. The extraction of the maxima at low surface coverage is the main drawback, and the Levenberg–Marquardt least squares minimization technique to fit absorption spectra is a successful [28]. A-SEC, absorption spectroelectrochemistry; PDI, perylenediimide; SAM, self-assembled monolayer; TBAHP, tetrabutylammonium hexafluorophosphate.

to 1650 nm) and the type of CCD camera (*i.e.* visible or NIR), the detection limit value varies between 10^{-5} and 10^{-3}.

The impact of nanoscale grafting such as the molecular structure change and/or an increase in intermolecular interactions can be studied by comparing A-SEC data in solution with those recorded on confined species. Hence, A-SEC performed on PDI-based SAMs did not provide evidence of significant spectral change for the confined PDI derivative and its reduced forms.

The grafting impact on the photoluminescence of PDI moieties has also been studied by E-SEC, and as expected, no light emission was detected because of quenching of molecular fluorescence on the Au substrate via an energy transfer (*i.e.* Förster resonance energy transfer). [26,27,29].

Grafting impact on EDIM mechanism

A-SEC at the nanoscale enables the study of the grafting impact on heterogeneous reactions coupled to charge transfer. In this context, the initial work aimed at probing the grafting impact on electrochemical reaction followed by a dimerization reaction (EDIM) mechanism.

Some short thiophene or thienylenevinylene derivatives are known to produce a reversible dimerization of the radical cation, leading to a π-dimer. In nonaqueous solvents, fully reversible EDIM and EDIM followed by an electrochemical reaction mechanisms were established via an expected linear dependence of apparent potential with log (C) (*i.e.* a slope of ± 29 mV/log unit at 293 K), and the equilibrium constant of dimerization (K_{DIM}) is greater than 10^4. Consequently, the absorption bands of the cation radical and π-dimer were identified from a systematic A-SEC study as a function of concentration (Figure 5 a) [30–34].

A-SEC study of 5,5′-disubstituted-2,2′-bithiophene–based SAMs (*i.e.* EDIM mechanism) provided evidence of the π-dimer optical signatures because of an expected increase of intermolecular interactions in confined nanometre-scale spaces (Figure 5 b). [35,36].

Electrochemical and spectroelectrochemical studies on mixed SAMs of a 2,5-bis(methylthio)-

Figure 5

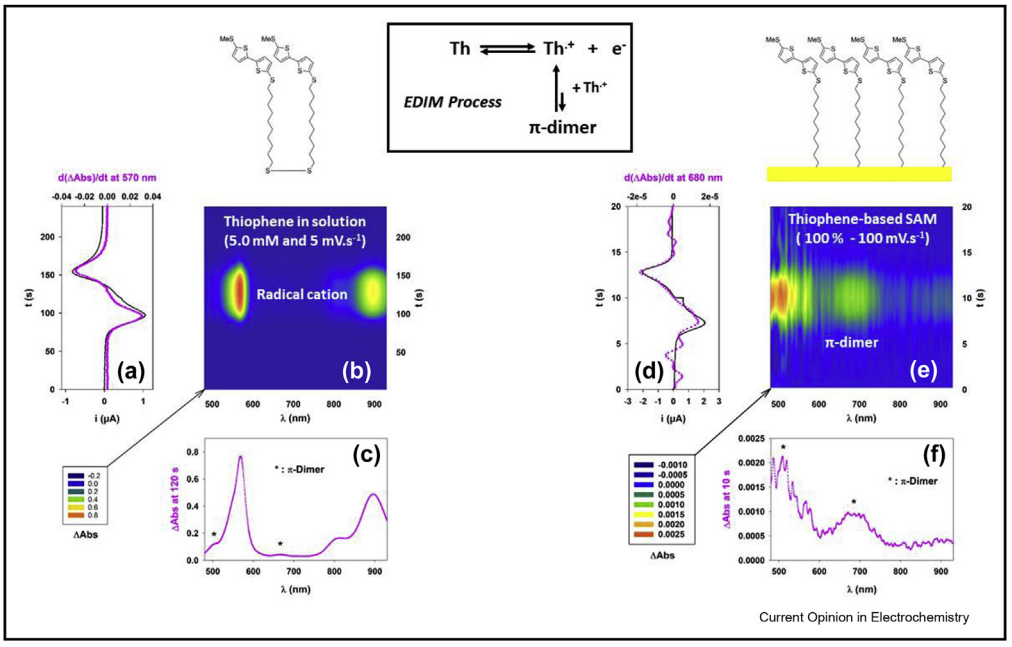

Electrochemical behaviour of a 5,50-disubstituted-2,20-bithiophene in 0.1 M TBAHP/CH_2Cl_2, involving a EDIM process in a positive direction (top). EDIM process supports by a linear variation of the apparent potential with log(c) (i.e. a slope of –29 mV/log unit). The invariance of apparent potentials with a scan rate between 0.10 and 100 V s^{-1} indicates that the dimerization equilibrium is fast. A-SEC experiment performed in solution and investigated at several concentrations does not provide clear evidence of the development of the characteristic spectral features of the π-dimer in the visible region. A-SEC experiment on thiophene-based SAMs has shown that the confinement of thiophene moieties on the Au substrate favours intermolecular interactions and thereby the formation of π-dimer. (a) Current vs. time and DCVA at 570 nm in thin layer conditions ($\ell \approx 50$ mm, C = 1 mM in 0.1 M TBAHP/CH_2Cl_2 on Pt electrode at 5 mV s^{-1}). (b) A-SEC response at a sampling rate of 5 Hz. (c) Absorbance variation of A-SEC response at 120 s. (d) Current vs. time and DCVA at 680 nm of a thiophene-based SAM ($\Gamma \approx 2\ 10^{-10}$ mol cm^{-2} in 0.1 M TBAHP/CH_2Cl_2 on Pt electrode at 50 mV s^{-1}). (e) A-SEC response at a sampling rate of 100 Hz. (f) Absorbance variation of A-SEC response at 10 s. Note that a colour scale represents the 3D graph z-axis. [35,37]. A-SEC, absorption spectroelectrochemistry; PDI, perylenediimide; SAM, self-assembled monolayer; TBAHP, tetrabutylammonium hexafluorophosphate; EDIM, electrochemical reaction followed by a dimerization reaction.

thienylenevinylene dialkyl disulfide derivative and dodecanethiol were provided to study the surface coverage impact on the EDIME process [37]. In agreement with electrochemical simulations performed with KISSA-1D© software [38], electrochemical data have suggested a conservation of the EDIME process for immobilized molecules. Then, A-SEC studies have confirmed the predominance of the π-dimer in a wide range of surface coverage (*i.e.* a dilution factor of 20). Nevertheless, the emergence of the signature of the radical cation has been monitored at low surface coverage by chronoamperometry coupled to absorption spectroscopy.

These first results suggest that a SAM could be seen as a high concentrated solution but that is to be confirmed through studying various electrochemical mechanisms.

Conclusion

Only a very few studies are dedicated so far to real-time A-SEC on SAMs in the literature because such equipment is very expensive and requires numerous repetitive and time-consuming fine adjustments. Nevertheless, a real-time A-SEC devoted to very low absorbance measurements is undoubtedly an asset for examining a more thorough electrochemical mechanism in solution (*e.g.* see study by Cotelle et al [39]) within redox-responsive materials (*e.g.* see the study by Jimenez et al [40]) or in surface-confined redox species [27,28,35,37], and it should facilitate the establishment of detailed structure properties and structure—reactivity relationships at the nanoscale. Finally, it is important to bear in mind that a fine study of current voltage characteristics, supported, where possible, by efficient electrochemical simulations (*e.g.* DigiElch or KISSA-1D©), should be initiated before performing A-SEC experiments on electroactive molecules in solution or on redox-responsive materials.

What about the real-time A-SEC future? The improvement in CCD cameras (*e.g.* deep depletion back-illuminated CCD cameras) and light sources (*e.g.* laser-driven light sources that enable extreme high brightness with a relatively flat spectrum, from UV to NIR) paves the way for better signal-to-noise ratios and smaller time scale monitoring in a few years. However, it

is likely that signal processing will bring about a huge improvement. Indeed, rapid advances in facial recognition have enhanced the alternating least squares algorithm for principal component analysis, opening up a whole range of possibilities for extracting very weak spectroscopic signals from noise. [41,42].

Conflict of interest

Nothing declared.

Acknowledgements

The authors thank Hellma® Analytics and Princeton Instruments companies for the quality of their products and their technical assistance and the "Contrat Plan État Région" 2007–2013 and 2014–2020 (Pays de la Loire, France, Europe) for the financial support. The authors thank Yohann Morille for his expertise in Matlab® programming and Clément Cabanetos for his critical reading of the manuscript.

References

Papers of particular interest, published within the period of review, have been highlighted as:

- • of special interest

1. Blubaugh EA, Yacynych AM, Heineman WR: **Thin-layer spectroelectrochemistry for monitoring kinetics of electrogenerated species**. *Anal Chem* 1979, **51**:561–565.

2. Pruiksma R, McCreery RL: **Observation of electrochemical concentration profiles by absorption spectroelectrochemistry**. *Anal Chem* 1979, **51**:2253–2257.

3. Skully JP, McCreery RL: **Glancing incidence external reflection spectroelectrochemistry with a continuum source**. *Anal Chem* 1980, **52**:1885–1889.

4. Robinson RS, McCreery RL: **Absorption spectroelectrochemistry with microelectrodes**. *Anal Chem* 1981, **53**: 997–1001.

5. Robinson RS, McCurdy CW, McCreery RL: **Microsecond spectroelectrochemistry by external reflection from cylindrical microelectrodes**. *Anal Chem* 1982, **54**:2356–2361.

6. Bard AJ, Faulkner LR: *Electrochemical methods: fundamentals and applications*. Wiley; 2000.

7. Kaim W, Klein A: *Spectroelectrochemistry*. Royal Society of Chemistry; 2008.

8. Kaim W, Fiedler J: **Spectroelectrochemistry: the best of two worlds**. *Chem Soc Rev* 2009, **38**:3373–3382.

9. • Dunsch L: **Recent Advances in in situ multi-spectroelectrochemistry**. *J Solid State Electrochem* 2011, **15**:1631–1646.
Extensive outline of *in situ* multi-spectroelectrochemistry

10. • Kuwana T, Darlington RK, Leedy DW: **Electrochemical studies using conducting Glass indicator electrodes**. *Anal Chem* 1964, **36**:2023–2025.
The pioneering work of real-time absorption specroelectrochemistry: a must-read!

11. León L, Mozo JD: **Designing spectroelectrochemical cells: a review**. *Trac Trends Anal Chem* 2018, **102**:147–169.

12. de Witte PAJ, Hernando J, Neuteboom EE, van Dijk E, Meskers SCJ, Janssen RAJ, van Hulst NF, Nolte RJM, Garcia-Parajo MF, Rowan AE: **Synthesis and characterization of long perylenediimide polymer fibers: from bulk to the single-molecule level**. *J Phys Chem B* 2006, **110**:7803–7812.

13. Zheng Y, Giordano AJ, Shallcross RC, Fleming SR, Barlow S, Armstrong NR, Marder SR, Saavedra SS: **Surface modification of indium tin oxide with functionalized perylene diimides: characterization of orientation, electron-transfer kinetics and electronic structure**. *J Phys Chem C* 2016, **120**: 20040–20048.

14. Hasegawa T, Takeda S, Kawaguchi A, Umemura J: **Quantitative-analysis of uniaxial molecular-orientation in Langmuir-Blodgett-Films by infrared reflection spectroscopy**. *Langmuir* 1995, **11**:1236–1243.

15. Hasegawa T, Ushiroda Y, Kawaguchi M, Kitazawa Y, Nishiyama M, Hiraoka A, Nishijo J: **UV absorption spectroscopic analysis of the molecular orientation of a drug penetrated into a DPPC membrane**. *Langmuir* 1996, **12**: 1566–1571.

16. Bramblett AL, Boeckl MS, Hauch KD, Ratner BD, Sasaki T, Rogers JW: **Determination of surface coverage for tetraphenylporphyrin monolayers using ultraviolet visible absorption and x-ray photoelectron spectroscopies**. *Surf Interface Anal* 2002, **33**:506–515.

17. Tang TJ, Qu JQ, Mullen K, Webber SE: **Molecular layer-by-layer self-assembly of water-soluble perylene diimides through pi-pi and electrostatic interactions**. *Langmuir* 2006, **22**:26–28.

18. Park HJ, So MC, Gosztola D, Wiederrecht GP, Emery JD, Martinson ABF, Er S, Wilmer CE, Vermeulen NA, Aspuru-Guzik A, *et al.*: **Layer-by-Layer assembled films of perylene diimide- and squaraine-containing metal-organic framework-like materials: solar energy capture and directional energy transfer**. *ACS Appl Mater Interfaces* 2016, **8**:24983–24988.

19. Schreiber F: **Structure and growth of self-assembling monolayers**. *Prog Surf Sci* 2000, **65**:151–256.

20. Zwahlen M, Tosatti S, Textor M, Hahner G: **Orientation in methyl- and hydroxyl-terminated self-assembled alkanephosphate monolayers on titanium oxide surfaces investigated with soft X-ray absorption**. *Langmuir* 2002, **18**: 3957–3962.

21. Gupta P, Ulman A, Fanfan S, Korniakov A, Loos K: **Mixed self-assembled monolayers of alkanethiolates on ultrasmooth gold do not exhibit contact-angle hysteresis**. *J Am Chem Soc* 2005, **127**:4–5.

22. Dias M, Hudhomme P, Levillain E, Perrin L, Sahin Y, Sauvage FX, Wartelle C: **Electrochemistry coupled to fluorescence spectroscopy: a new versatile approach**. *Electrochem Commun* 2004, **6**:325–330.

23. • Audebert P, Miomandre F: **Electrofluorochromism: from molecular systems to set-up and display**. *Chem Sci* 2013, **4**: 575–584.
A didactic reference of setups dedicated to electrofluorochromism.

24. Gaillard F, Levillain E: **Visible time-resolved spectroelectrochemistry - application to study of the reduction of sulfur (S-8) in dimethylformamide**. *J Electroanal Chem* 1995, **398**:77–87.

25. Alévêque O, Levillain E: **Emission spectroelectrochemistry**. In *Luminescence in electrochemistry: applications in analytical chemistry, physics, and biology*, vol 1. Springer; 2015:1–19.

26. • Bizzotto D: **In situ spectroelectrochemical fluorescence microscopy for studying electrodes modified by molecular adsorbates**. *Curr Opin Electrochem* 2018, **7**:161–171.
A comprehensive reference of emission spectroelectrochemsitry on self-assembled monolayers

27. Bkhach S, Le Duc Y, Aleveque O, Gautier C, Hudhomme P, Levillain E: **Highly stable perylenediimide based self-assembled monolayers studied by spectroelectrochemistry**. *Chem Electro Chem* 2016, **3**:887–891.

28. • Bkhach S, Aleveque O, Morille Y, Breton T, Hudhomme P, Gautier C, Levillain E: **Absorption spectroelectrochemistry on mixed perylenediimide-based self-assembled monolayers: non-linear dependence of absorbance versus surface coverage**. *Chem Electro chem* 2017, **4**:601–606.
An overview of real-time absorption spectroelectrochemistry on perylene-based SAMs.

29. Casanova-Moreno JR, Bizzotto D: **What happens to the thiolates created by reductively desorbing SAMs? An in situ study using fluorescence microscopy and electrochemistry**. *Langmuir* 2013, **29**:2065–2074.

30. Neudeck A, Audebert P, Guyard L, Dunsch L, Guiriec P, Hapiot P: **pi-dimer from bithiophene radical cations. Investigation of equilibrium constants as a function of substituent size and**

supporting electrolyte using fast conversion electrochemical cells. *Acta Chem Scand* 1999, **53**:867–875.

31. Levillain E, Roncali J: **Structural control of the reversible dimerization of pi-conjugated oligomeric cation radicals**. *J Am Chem Soc* 1999, **121**:8760–8765.

32. Amatore C, Garreau D, Hammi M, Pinson J, Saveant JM: **Kinetic-analysis of reversible electrodimerization reactions by the combined use of double potential step chronoamperometry and linear sweep voltammetry - application to the reduction of 9-cyanoanthracene**. *J Electroanal Chem* 1985, **184**:1–24.

33. Audebert P, Hapiot P, Pernaut JM, Garcia P: **Electrochemical reactivity of the oxidized species of thiophene oligomers - formal oxidation potential of alpha-bromo-alpha(')-methoxy-quaterthienyl**. *J Electroanal Chem* 1993, **361**:283–287.

34. Hapiot P, Audebert P, Monnier K, Pernaut JM, Garcia P: **Electrochemical evidence of pi-dimerization with short thiophene oligomers**. *Chem Mater* 1994, **6**:1549–1555.

35. Aleveque O, Levillain E, Sanguinet L: **Spectroelectrochemistry on electroactive self-assembled monolayers: cyclic voltammetry coupled to spectrophotometry**. *Electrochem Commun* 2015, **51**:108–112.

36. Trasobares J, Rech J, Jonckheere T, Martin T, Aleveque O, Levillain E, Diez-Cabanes V, Olivier Y, Cornil J, Nys JP, *et al.*: **Estimation of pi-pi electronic couplings from current measurements**. *Nano Lett* 2017, **17**:3215–3224.

37. Bkhach S, Aleveque O, Blanchard P, Gautier C, Levillain E: **Thienylene vinylene dimerization: from solution to self-assembled monolayer on gold**. *Nanoscale* 2018, **10**: 1613–1616.

38. • Amatore C, Klymenko O, Svir I: **A new strategy for simulation of electrochemical mechanisms involving acute reaction fronts in solution: principle**. *Electrochem Commun* 2010, **12**: 1170–1173.
The reference of KISSA-1D© software: a robust electrochemical simulator for simulating an electrochemical behaviour of redox confined species.

39. Cotelle Y, Hardouin-Lerouge M, Legoupy S, Alévêque O, Levillain E, Hudhomme P: **Glycoluril–tetrathiafulvalene molecular clips: on the influence of electronic and spatial properties for binding neutral accepting guests**. *Beilstein J Org Chem* 2015, **11**:1023–1036.

40. Jimenez P, Levillain E, Aleveque O, Guyomard D, Lestriez B, Gaubicher J: **Lithium n-doped polyaniline as a high-performance electroactive material for rechargeable batteries**. *Angew Chem Int Ed Engl* 2017, **56**:1553–1556.

41. Kuroda M, Mori Y, Iizuka M, Sakakihara M: **Acceleration of the alternating least squares algorithm for principal components analysis**. *Comput Stat Data Anal* 2011, **55**:143–153.

42. Jaumot J, de Juan A, Tauler R: **Mcr-als gui 2.0: new features and applications**. *Chemometr Intell Lab Syst* 2015, **140**:1–12.